

# Comment on “Directed motion of spheres by unbiased driving forces in viscous fluids beyond the Stokes’ law regime”

Pedro J. Martínez<sup>1</sup> and Ricardo Chacón<sup>2</sup>

<sup>1</sup>*Instituto de Nanociencia y Materiales de Aragón (INMA),  
CSIC-Universidad de Zaragoza, E-50009 Zaragoza,  
Spain and Departamento de Física Aplicada, E.I.N.A.,  
Universidad de Zaragoza, E-50018 Zaragoza, Spain and*

<sup>2</sup>*Departamento de Física Aplicada, E.I.I., Universidad de Extremadura, Apartado Postal 382,  
E-06006 Badajoz, Spain, and Instituto de Computación Científica Avanzada (ICCAEx),  
Universidad de Extremadura, E-06006 Badajoz, Spain*

(Dated: October 20, 2021)

In a recent paper by Casado-Pascual [Phys. Rev. E **97**, 032219 (2018)], directed motion of a sphere immersed in a viscous fluid and subjected to zero-average biharmonic forces is studied. The author explains the dependence on the relative amplitude of the two harmonic components of the average terminal velocity from the perspective of a general formalism. In this Comment, this explanation is shown to be in general incorrect, while the theory of ratchet universality together with the vibrational mechanics approach provide a satisfactory explanation of major aspects of the observed phenomena.

PACS numbers:

Motivated by investigation into the effects of non-linear dissipative (drag) forces on directed ratchet motion in the absence of any periodic substrate potential, Casado-Pascual [1] has studied theoretically and numerically spheres immersed in a viscous fluid and subjected to time-periodic forces of zero average. In dimensionless variables, the equation of motion reads

$$\omega\tau \frac{d\mathbf{v}(\theta)}{d\theta} = -\frac{1}{24}C_d [|\mathbf{v}(\theta)|] |\mathbf{v}(\theta)| \mathbf{v}(\theta) + f_0 \mathbf{f}(\theta), \quad (1)$$

$$\mathbf{f}(\theta) = \zeta \cos(\theta) \mathbf{e}_1 + \alpha(1 - \zeta) \cos(2\theta + \varphi) \mathbf{e}_2, \quad (2)$$

where  $\theta \equiv \omega t$ ,  $\tau \equiv m/(6\pi r\eta)$  is a characteristic timescale,  $\mathbf{v}(\theta) \equiv 2r\rho_f \mathbf{v}(\theta/\omega)/\eta$ ,  $C_d [|\mathbf{v}(\theta)|]$  is the steady drag coefficient,  $f_0$  is a dimensionless parameter accounting for the strength of the driving force,  $\mathbf{e}_1$  and  $\mathbf{e}_2$  are two mutually perpendicular versors,  $\zeta \in [0, 1]$  and  $\varphi \in [0, 2\pi]$  account for the relative amplitude and initial phase difference of the two harmonic components, respectively, while the value  $\alpha = 1$  is the only one considered in Ref. [1]. In the adiabatic limit ( $\omega\tau \ll 1$ ), the average terminal velocity,  $\bar{\mathbf{V}}_{ad}$ , is given by the integral

$$\bar{\mathbf{V}}_{ad} = \frac{\delta_0^2 \eta}{16\pi r \rho_f} \int_0^{2\pi} d\theta \left[ \sqrt{1 + \frac{4\sqrt{f_0} |\mathbf{f}(\theta)|}{\delta_0}} - 1 \right]^2 \frac{\mathbf{f}(\theta)}{|\mathbf{f}(\theta)|}, \quad (3)$$

with  $\delta_0 = 9.06$  [1].

Commenting on Fig. 3 of Ref. [1] (second component of the dimensionless average terminal velocity versus  $\zeta$ ), the author claims that: “The curves in Fig. 3 also reveal that, for fixed values of the other parameters, there exists an optimal value of  $\zeta$  which maximizes the second component of the average terminal velocity. Furthermore, as  $\omega\tau$  increases, the maximum velocity decreases and its location shifts toward lower values of  $\zeta$ . It should be noted here that, in the lowest order, the general formalism developed in Refs. [27,28] [for Refs. [2,3]] leads to the

approximate expression  $\bar{V}_2(\zeta) \approx C\zeta^2(1 - \zeta)$ , where  $C$  is independent of  $\zeta$ . This expression vanishes at  $\zeta = 0$  and  $\zeta = 1$ , and displays a maximum at  $\zeta = 2/3$ , thus qualitatively resembling the behavior seen in Fig. 3. However, it is unable to account for the dependence of the location of the maximum velocity on  $\omega\tau$ . This deficiency is not surprising, given that the above approximation is expected to be accurate only for small values of  $f_0$  and, in Fig. 3, we have taken  $f_0 = 100$ .”

This Comment will question some of the above statements. For any  $\alpha > 0$ , we shall argue that the maximum velocity is reached for  $\zeta = 2\alpha/(1 + 2\alpha)$  as predicted by the theory of ratchet universality (RU) [4-6]. Indeed, it has been demonstrated for temporal and spatial biharmonic forces that optimal enhancement of directed ratchet transport is achieved when maximally effective (i.e., *critical*) symmetry breaking occurs, which implies the existence of a particular universal waveform [4-6]. Specifically, the optimal value of the relative amplitude  $\zeta$  comes from the condition that the amplitude of the odd harmonic component must be twice that of the even harmonic component in Eq. (2), i.e.,

$$\zeta_{opt} = \zeta_{opt}(\alpha) \equiv 2\alpha/(1 + 2\alpha). \quad (4)$$

Note that this finding is in sharp contrast with the prediction coming from the aforementioned general formalism [2,3], namely, that the dependence of the average terminal velocity should scale as

$$\bar{V}_2(\zeta) \approx C\zeta^2\alpha(1 - \zeta). \quad (5)$$

Equation (5) indicates that  $\bar{V}_2(\zeta)$  presents again a single maximum at  $\zeta_{opt} = 2/3$ , *irrespective* of the particular value of the prefactor  $\alpha$ . In contrast, both the theoretical estimate given by Eq. (3) and numerical simulations of Eq. (1) confirm the RU prediction [Eq. (4)] over a wide

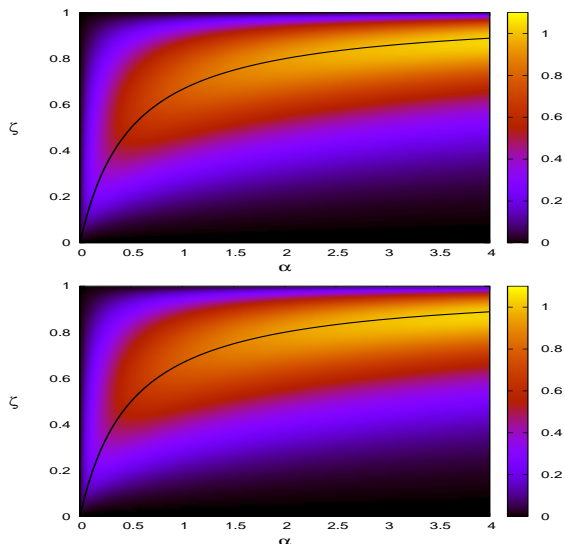


FIG. 1: Dimensionless average terminal velocity versus relative amplitude  $\zeta$  and prefactor  $\alpha$  [cf. Eq. (2)] for  $f_0 = 100$ ,  $\omega\tau = 0.1$ , and  $\varphi = \pi$ . Top: Theoretical prediction from Eq. (3). Bottom: Numerical results from Eqs. (1) and (2). Also plotted is the theoretical prediction for the maximum velocity [cf. Eq. (4); solid curve].

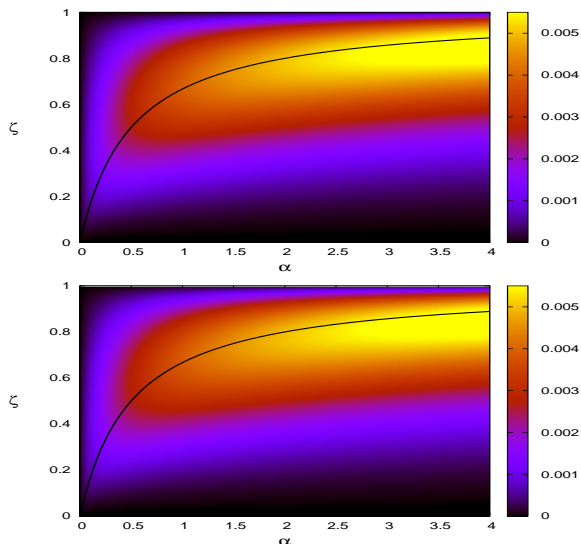


FIG. 2: The same as Fig. 1, but now  $f_0 = 1$ .

range of  $\alpha$  values (cf. Figs. 1 top and bottom, respectively).

Figure 2 is the same as Fig. 1 but for a much lower dimensionless driving strength ( $f_0 = 1$ ). One sees that the theoretical estimate given by Eq. (3) and numerical simulations of Eq. (1) again confirm the RU prediction [Eq. (4)] over the same range of  $\alpha$  values (cf. Figs. 2 top and bottom, respectively). Note that the average terminal velocity increases as the prefactor  $\alpha$  is increased, while keeping the remaining parameters constant (cf. Figs. 1 and 2), because the condition  $|\mathbf{f}(\theta)| \leq 1$

is no longer satisfied for  $\alpha > 1$  and the particular value of  $F_0$  considered in Ref. [1] for  $\alpha = 1$ .

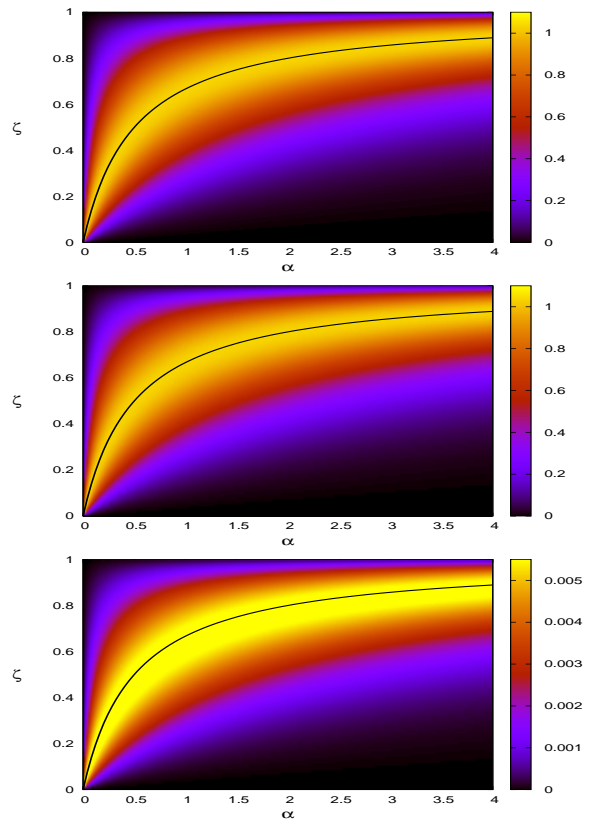


FIG. 3: Dimensionless average terminal velocity versus relative amplitude  $\zeta$  and prefactor  $\alpha$  [cf. Eq. (2)] for  $\omega\tau = 0.1$ ,  $\varphi = \pi$ , and  $F_0$  such that  $|\mathbf{f}(\theta)| \leq 1$ . Top: Theoretical prediction from Eq. (3) for  $f_0 = 100$ . Middle: Numerical results from Eqs. (1) and (2) for  $f_0 = 100$ . Bottom: Numerical results from Eqs. (1) and (2) for  $f_0 = 1$ . Also plotted is the theoretical prediction for the maximum velocity [cf. Eq. (4); solid curve].

For the sake of making a legitimate comparison, Fig. 3 shows the corresponding results after choosing the suitable value of  $F_0 \equiv \sqrt{\zeta^2 + \alpha^2(1 - \zeta)^2}$  such that  $|\mathbf{f}(\theta)| \leq 1$ . Clearly, the RU prediction presents excellent agreement with the results from numerical simulations for quite disparate values of  $f_0$  (cf. Figs. 3 middle and bottom) as well as with the theoretical estimate [Eq. (3); Fig. 3 top]. The effectiveness of the RU prediction [Eq. (4)] can be understood as follows. In the adiabatic limit ( $\omega\tau \ll 1$ ), after substituting Eq. (11) of Ref. [1] into the expression  $C_d[|\mathbf{v}_{ad}(\theta)|]|\mathbf{v}_{ad}(\theta)|\mathbf{v}_{ad}(\theta)$  with the assumption  $\mathbf{v}_{ad}(\theta) \approx \mathbf{f}(\theta)$ , and Taylor- and Fourier-expanding the nonlinear part of this friction force, for

instance for  $\varphi = \varphi_{opt} \equiv \pi$ , Eq. (1) can be written as

$$\omega\tau \frac{dv_1}{d\theta} = -v_1 - A \sum_{n=1}^{\infty} b_{2n-1} \cos[(2n-1)\theta] + f_0 \zeta \cos \theta, \quad (6)$$

$$\omega\tau \frac{dv_2}{d\theta} = -v_2 - A \sum_{n=0}^{\infty} a_{2n} \cos(2n\theta) - f_0 \alpha (1 - \zeta) \cos(2\theta), \quad (7)$$

where  $A \equiv A(\delta_0, f_0)$  and the Fourier coefficients  $a_{2n} \equiv a_{2n}(\zeta, \alpha)$ ,  $b_{2n-1} \equiv b_{2n-1}(\zeta, \alpha)$  can be calculated explicitly by using MATHEMATICA, but their size and algebraic complexity prevent us from showing them eas-

ily. One sees that the net periodic force in Eq. (6) only presents odd harmonics and hence satisfies the shift symmetry, which means that, as expected from the symmetry analysis in Ref. [1], such a periodic force by itself cannot yield directed ratchet motion in the  $\mathbf{e}_1$  direction. Also, the net force in Eq. (7) only presents even harmonics and a constant force term

$$-Aa_0 \approx \sum_{k=0}^{\infty} \sum_{n=0}^k \frac{\binom{k}{n} \zeta^{2k-2n} \alpha^{2n+1} (1-\zeta)^{2n+1} c(k, n)}{\Gamma\left(\frac{1}{8} - k + 1\right) k! \left[\zeta^2 + \alpha^2 (1-\zeta)^2\right]^k}, \quad (8)$$

with

$$\frac{c(k, n)}{\Delta_{k, n}} \equiv \sqrt{\pi} {}_2\tilde{F}_1\left(\frac{1}{2}, \frac{k+n+3}{2}; n + \frac{3}{2}; -1\right) + (-1)^n {}_2\tilde{F}_1\left(\frac{k-n+2}{2}, \frac{k+n+3}{2}; \frac{k+n+4}{2}; -1\right) \Gamma\left(\frac{k-n+2}{2}\right), \quad (9)$$

where  $\Delta_{k, n} \equiv (-1)^{-n} \left[(-1)^n - (-1)^k\right] \Gamma(n+1)$  while  $\Gamma(\cdot)$  and  ${}_2\tilde{F}_1(\cdot, \cdot; \cdot; \cdot)$  are the gamma and the regularized hypergeometric functions, respectively. Since the waveform of any pair of even harmonics  $a_{2n} \cos(2n\theta) + a_{2n+2} \cos[(2n+2)\theta]$  in Eq. (7) does not fit, for any value of  $\zeta, \alpha$ , that of one of the four equivalent expressions of the biharmonic universal excitation [4]

$$\begin{aligned} f_0 \left[ \sin \theta \pm \frac{1}{2} \sin(2\theta) \right], \\ f_0 \left[ \cos \theta \pm \frac{1}{2} \sin(2\theta) \right], \end{aligned} \quad (10)$$

this means that the emergence of directed ratchet motion in the  $\mathbf{e}_2$  direction is exclusively due to the constant force  $-Aa_0$  which is given approximately by Eq. (8) for the parameters used in Fig. 3 of Ref. [1]. Indeed, the RU prediction [Eq. (4)] presents good agreement with the theoretical estimate of the constant force arising from the Fourier analysis of the net force [cf. Eq. (8); see Fig. 4] because the universal biharmonic waveform is effectively present to produce the term of constant force *once*  $\mathbf{f}(\theta)$  has been suitably normalized as in the criticality scenario leading to ratchet universality [5].

Next, the aforementioned “dependence of the location of the maximum velocity on  $\omega\tau$ ” (cf. Ref. [1]) can be understood as follows. First, we rewrite Eq. (1) as

$$\begin{aligned} \frac{d\mathbf{v}(\Omega t_\tau)}{dt_\tau} = & -\frac{1}{24} C_d [|\mathbf{v}(\Omega t_\tau)|] |\mathbf{v}(\Omega t_\tau)| \mathbf{v}(\Omega t_\tau) \\ & + f_0 [\zeta \cos(\Omega t_\tau) \mathbf{e}_1 + \alpha (1 - \zeta) \cos(2\Omega t_\tau + \varphi) \mathbf{e}_2], \end{aligned} \quad (11)$$

where  $\Omega \equiv \omega\tau$ ,  $t_\tau \equiv t/\tau$ . For sufficiently large  $\Omega$ , i.e., when  $\tau \gtrsim T$ , the  $v_2$  dynamics of Eq. (11) can be anal-

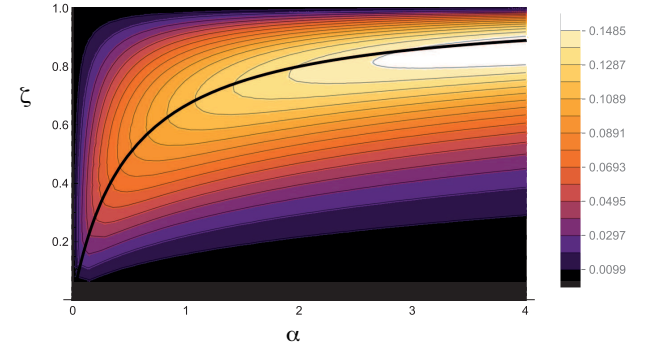


FIG. 4: Estimation of the constant term  $-Aa_0$  after retaining only the first six terms versus relative amplitude  $\zeta$  and prefactor  $\alpha$  [cf. Eq. (8)] for  $f_0 = 100$ . Also plotted is the theoretical prediction for the maximum velocity [cf. Eq. (4); solid curve].

ysed using the vibrational mechanics approach [7] by assuming that the  $\Omega$ -force is “slow” while the  $2\Omega$ -force is “fast”. Thus, one separates  $v_2(t_\tau) = V_2(t_\tau) + \psi(t_\tau)$ , where  $V_2(t_\tau)$  represents the slow dynamics while  $\psi(t_\tau)$  is the fast oscillating term:  $\psi(t_\tau) = \psi_0 \cos(2\Omega t_\tau + \Phi)$  with  $\psi_0 \equiv f_0 \alpha (1 - \zeta) / \sqrt{1 + 4\Omega^2}$ ,  $\Phi \equiv \arctan\left[\frac{t g \varphi - 2\pi}{1 + 2\Omega t g \varphi}\right]$ . On averaging out  $\psi(t_\tau)$  over time  $2\Omega t_\tau$ , the slow reduced dynamics of  $v_2$  becomes

$$\frac{dV_2}{dt_\tau} = -V_2 + \frac{4\pi}{\delta_0} V_2^{3/2}. \quad (12)$$

Thus, the asymptotic  $v_2$  dynamics when  $\Omega \equiv \omega\tau \gg 1$  could well be described by Eq. (12), which indicates that the (terminal) velocity  $V_2 \sim e^{-t/\tau}$  as  $t \rightarrow \infty$ . This scenario is coherent with the gradual decrease of the maxi-

imum second component of the dimensionless average terminal velocity (cf. Fig. 3 in Ref. [1]) as  $\omega\tau$  is increased from the adiabatic limit, i.e., as the relevant symmetries are gradually restored. This phenomenon of competing timescales leads to the  $2\Omega$ -force losing ratchet effectiveness, but without deactivating the degree-of-symmetry-breaking mechanism [4,5]. Clearly, this loss of effectiveness can only be compensated by increasing its amplitude  $\alpha(1 - \zeta)$  to generate maximum velocity, thereby explaining the shift of the location of the maximum velocity to lower values of  $\zeta$  as  $\omega\tau$  is increased from the adiabatic limit (cf. Fig. 3 in Ref. [1]).

Finally, the author claims that: “In this class of models [for rocking ratchets in the presence of thermal noise], the mechanism behind the generation of directed motion is basically harmonic mixing... .” This is incorrect. It has been demonstrated that optimal enhancement of directed motion is achieved when maximal effective (i.e., critical)

symmetry breaking occurs [4,5], while the effect of finite temperature on the purely deterministic criticality scenario can be understood as an effective noise-induced change of the potential barrier which is in turn controlled by the degree-of-symmetry-breaking mechanism [8-10].

In conclusion, the theoretical explanation discussed in Ref. [1] is in general incorrect, while the theory of RU and the vibrational mechanics approach provide a satisfactory explanation of major aspects of the observed phenomena.

P.J.M. acknowledges financial support from the Ministerio de Economía y Competitividad (MINECO, Spain) through Project No. FIS2017-87519 cofinanced by FEDER funds and from the Gobierno de Aragón (DGA, Spain) through Grant No. E36\_17R to the FENOL group. R.C. acknowledges financial support from the Junta de Extremadura (JEx, Spain) through Project No. GR18081 cofinanced by FEDER funds.

- 
- [1] J. Casado-Pascual, Directed motion of spheres induced by unbiased driving forces in viscous fluids beyond the Stokes' law regime, *Phys. Rev. E* **97**, 032219 (2018).
- [2] J. A. Cuesta, N. R. Quintero, and R. Alvarez-Nodarse, Time-Shift Invariance Determines the Functional Shape of the Current in Dissipative Rocking Ratchets, *Phys. Rev. X* **3**, 041014 (2013).
- [3] J. Casado-Pascual, J. A. Cuesta, N. R. Quintero, and R. Alvarez-Nodarse, General approach for dealing with dynamical systems with spatiotemporal periodicities, *Phys. Rev. E* **91**, 022905 (2015).
- [4] R. Chacón, Optimal control of ratchets without spatial asymmetry, *J. Phys. A* **40**, F413 (2007).
- [5] R. Chacón, Criticality-induced universality in ratchets, *J. Phys. A* **43**, 322001 (2010).
- [6] R. Chacón and P. J. Martínez, Exact universal excitation waveform for optimal enhancement of directed ratchet transport, *Int. J. Bifurcation and Chaos* **31**, 2150109 (2021).
- [7] I. I. Blekhman, *Vibrational Mechanics* (World Scientific, Singapore, 2000).
- [8] P. J. Martínez and R. Chacón, Ratchet universality in the presence of thermal noise, *Phys. Rev. E* **87**, 062114 (2013).
- [9] P. J. Martínez and R. Chacón, Erratum: Ratchet universality in the presence of thermal noise [*Phys. Rev. E* **87**, 062114 (2013)], *Phys. Rev. E* **88**, 019902(E) (2013).
- [10] P. J. Martínez and R. Chacón, Reply to “Comment on ‘Ratchet universality in the presence of thermal noise’”, *Phys. Rev. E* **88**, 066102 (2013).